



Heat capacities of polycrystalline ${}^n\text{LiH}$ and ${}^n\text{LiD}$ by differential scanning calorimetric method

Ram Avtar Jat^a, S.C. Parida^{a,*}, K. Krishnan^b, N.S. Anand^a, S.G. Sawant^a, Renu Agarwal^a, Ziley Singh^a, S.K. Aggarwal^b, V. Venugopal^c

^a Product Development Division, Bhabha Atomic Research Centre, Trombay, Mumbai 400 085, India

^b Fuel Chemistry Division, Bhabha Atomic Research Centre, Trombay, Mumbai 400 085, India

^c RC & I Group, Bhabha Atomic Research Centre, Trombay, Mumbai 400 085, India

ARTICLE INFO

Article history:

Received 27 April 2010

Received in revised form 2 June 2010

Accepted 8 June 2010

Available online 16 June 2010

Keywords:

Lithium hydride

Heat capacity

Differential scanning calorimetry

Thermodynamic functions

Isotopic effect

ABSTRACT

The heat capacities of polycrystalline ${}^n\text{LiH}$ and ${}^n\text{LiD}$ were measured by differential scanning calorimeter in the temperature range from 125 to 800 K. The smoothed values of heat capacities were used to calculate various thermodynamic functions for ${}^n\text{LiH}$ and ${}^n\text{LiD}$ from 0 to 800 K. Isotopic effect on heat capacity of ${}^n\text{LiH}$ and ${}^n\text{LiD}$ is predominant at higher temperatures (>80 K) whereas below 80 K the isotopic effect is negligible.

© 2010 Elsevier B.V. All rights reserved.

1. Introduction

Lithium hydride is a very important technological material [1] with great scientific interest for fundamental understanding of lattice dynamics. It crystallizes in NaCl-type structure and presumably an ionic material consisting of Li^+ and H^- ions. The large relative mass difference between the isotopes and its low reduced mass makes its lattice properties amenable to significant changes with isotopic substitution. Excellent accounts of research on isotope effects on lattice dynamics of LiH and LiD have been published in several review articles [2–5]. Extensive studies on elastic parameters [6–11], lattice parameters and thermal expansion coefficients [11–22], specific heats and Debye temperatures [21–31] have been carried out both for LiH and LiD by many investigators. Experimental and theoretical investigation on the other physico-chemical properties of isotopic lithium hydride has been carried out by many researchers [16–18,20,32–44]. However, these studies are limited to narrow temperature ranges, preferably sub-ambient temperatures and on single crystals. Comprehensive work on measurement of heat capacity of ${}^n\text{LiH}$ and ${}^n\text{LiD}$ (where n represents natural lithium) at elevated temperatures is reported in Ref. [21]. Tabu-

lated values of heat capacity of LiH are reported in NIST-JANAF thermochemical tables [45]. The data reported in the above literatures show considerable scatter. To the best of author's knowledge, the high temperature heat capacity of LiD is not reported in the literature.

Therefore as a part of thermodynamic studies on binary and ternary compounds in the Li–N–H system for the development of solid-state hydrogen storage material, an effort is made in this work to measure the heat capacities of ${}^n\text{LiH}$ and ${}^n\text{LiD}$ from 125 to 800 K using differential scanning calorimeter in order to understand the isotopic effects.

2. Experimental

2.1. Sample preparation

${}^n\text{LiH}$ and ${}^n\text{LiD}$ materials (both 0.96 mass fraction purity), prepared at Bhabha Atomic Research Centre, were handled in a helium atmosphere glove box with moisture and oxygen content below ~ 1 ppm. The purity of glove box was maintained by conventional sacrificial molten sodium bath to getter the last traces of oxygen and moisture. For the measurement of heat capacity, the sample was loaded into aluminum sample container and crimped with aluminum cover with a hole at the centre, inside the glove box and then transferred to the differential scanning calorimeter.

2.2. Characterization of ${}^n\text{LiH}$ and ${}^n\text{LiD}$ using X-ray diffraction method

Owing to the hygroscopic nature of the sample, the X-ray diffraction measurements were carried out using a STOE diffractometer (theta–theta geometry), fitted with HDK-2.4 high temperature attachment, equipped with a high vacuum cham-

* Corresponding author at: Product Development Division, Bhabha Atomic Research Centre, Trombay, Mumbai 400 085, India. Tel.: +91 22 2559 0648; fax: +91 22 2550 5151.

E-mail address: sureshp@barc.gov.in (S.C. Parida).

ber maintained at a pressure of 1×10^{-5} mbar. The samples were mounted on Pt–Rh sample carrier; spot welded at the bottom with a Pt/Pt–13% Rh thermocouple for temperature measurement. The silicon and platinum standards were used to calibrate the instrument. The room temperature XRD patterns were recorded in the 2θ range of $20\text{--}85^\circ$, with 0.034° steps for 3 s counting time using $\text{Cu K}\alpha$ radiation with graphite monochromator ($\lambda = 1.5406 \text{ \AA}$). Lattice parameters of these materials were determined using the X-ray diffraction data and compared with the reported literature values.

2.3. Heat capacity by differential scanning calorimetry (DSC)

The heat flux DSC (Model: DSC 131) supplied by M/s. SETARAM Instrumentations, France, was used to measure the heat capacities of the samples. The transducer of DSC 131 has been designed using the technology of the plate-shaped DSC rods made of chromel–constantan. It is arranged in a small furnace with a metal resistor of low-thermal inertia so as to produce high heating and cooling rates, thereby providing for high-speed experiments. The transducer also possesses very good sensitivity over the whole temperature range (100–950 K). The temperature calibration of the calorimeter was carried out in the present study by the phase transition temperatures of NIST (National Institute of Standards and Technology) reference materials (mercury, gallium, indium, tin, lead) and AR grade samples (*n*-pentane, cyclohexane, deionised water, potassium nitrate, silver sulfate, potassium sulfate). Heat calibration of the calorimeter was carried out by using the enthalpies of transition of the above mentioned materials to check the sensitivity of DSC. For the determination of heat capacity, NIST synthetic sapphire (SRM 720) in the powder form was used as the reference material. Heat capacities were determined by the classical three-step method in the step heating mode in two different temperature ranges: (i) $125 \leq T/\text{K} \leq 325$ and (ii) $300 \leq T/\text{K} \leq 800$. Heat flow as a function of temperature was measured in the first temperature range at a heating rate of 5 K min^{-1} with high purity helium as a carrier gas with a flow rate of $2 \text{ dm}^3 \text{ h}^{-1}$. For the second temperature range, high purity argon was used as a carrier gas with the same flow rate as that of helium and same heating rate. Two flat bottom aluminum crucibles of identical masses of capacity 10^{-4} dm^3 with covering lids were used as containers for sample and reference materials. About 300–350 mg of the sample was used for the heat capacity measurements. The accuracy and reproducibility of measurements were checked by measuring the heat capacities of molybdenum (NIST) and found to be within $\pm 2\%$ of the literature values [45].

3. Results and discussion

3.1. Lattice parameters of ${}^n\text{LiH}$ and ${}^n\text{LiD}$

The samples of ${}^n\text{LiH}$ and ${}^n\text{LiD}$ prepared at Bhabha Atomic Research Centre were characterized by X-ray diffraction method described in Section 2.2. The room temperature X-ray diffraction patterns of ${}^n\text{LiH}$ and ${}^n\text{LiD}$ are shown in Fig. 1. These XRD patterns are used to calculate the lattice parameters of ${}^n\text{LiH}$ and ${}^n\text{LiD}$. The lattice parameters of ${}^n\text{LiH}$ and ${}^n\text{LiD}$ obtained in this study are compared with the literature values in Table 1 and found to be in excellent agreement. Furthermore, impurity peaks were not observed in the X-ray diffraction patterns which confirm that the materials are phase pure within the detection limit of X-ray diffraction method employed in this study.

3.2. Heat capacities of ${}^n\text{LiH}$ and ${}^n\text{LiD}$

The heat capacities of ${}^n\text{LiH}$ and ${}^n\text{LiD}$ obtained in the present study in both the temperature ranges: (i) 125–325 K and (ii) 300–800 K, are shown in Fig. 2 along with the reported low temperature values of ${}^7\text{LiH}$ and ${}^7\text{LiD}$ from 4–320 K [23] and it is evident that there is excellent agreement within $\pm 0.5\%$. The small deviation from reported literature values is attributed due to the differ-

Table 1
Lattice parameters (a in \AA) of LiH and LiD at 298 K.

LiH	LiD	Ref.
4.0826	4.0626	This study (error: $\pm 0.01\%$)
4.0829	4.0693	[13]
4.0845	4.0725	[16]
4.0831	4.0684	[12]
4.0856	–	[19]

This study is on ${}^n\text{LiH}$ and ${}^n\text{LiD}$; all other studies on ${}^7\text{LiH}$ and ${}^7\text{LiD}$.

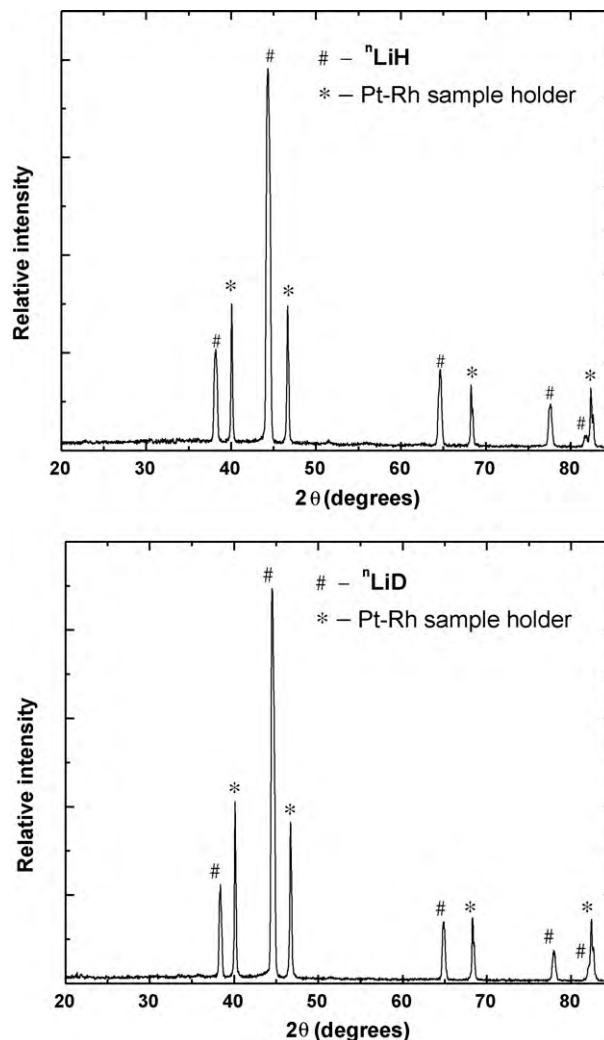


Fig. 1. Room temperature X-ray diffraction patterns of ${}^n\text{LiH}$ and ${}^n\text{LiD}$.

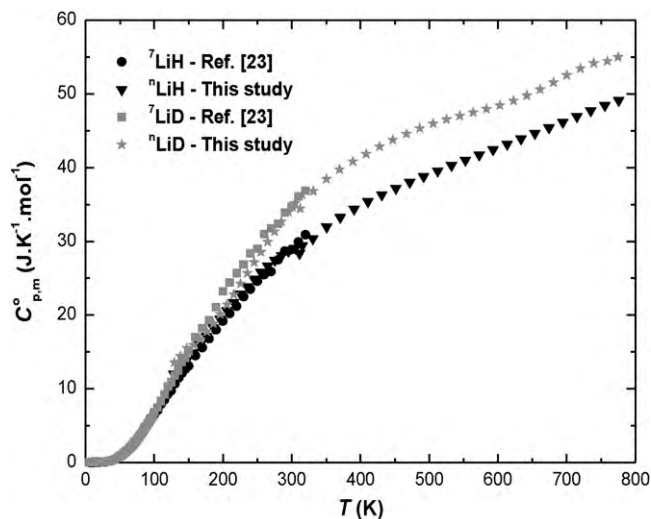


Fig. 2. Variation of heat capacities ($C_{p,m}^0$) of ${}^n\text{LiH}$ and ${}^n\text{LiD}$ as a function of temperature.

Table 2
Coefficients obtained from a fit of the experimental heat capacity with Eq. (1).

Parameters	Coefficients	
	^nLiH	^nLiD
m	1.198 ± 0.024	1.452 ± 0.047
n	0.4807 ± 0.024	0.5457 ± 0.044
Θ_D/K	1109 ± 13	1076 ± 17
Θ_E/K	359 ± 6	400 ± 10
$A_1/\text{J K}^{-2} \text{mol}^{-1}$	$1.194 \times 10^{-3} \pm 1.868 \times 10^{-4}$	$2.458 \times 10^{-3} \pm 9.208 \times 10^{-4}$
$A_2/\text{J K}^{-3} \text{mol}^{-1}$	$1.478 \times 10^{-5} \pm 3.923 \times 10^{-7}$	$1.063 \times 10^{-5} \pm 6.547 \times 10^{-7}$

ence in isotopic compositions of lithium. The heat capacity data in the entire range of temperature from 0 to 800 K can therefore be obtained by a least squares analysis of both the low temperature reported data and the data obtained in the present study within the limit of experimental accuracy. In order to calculate the smoothed heat capacity and thermodynamic functions, Woodfield et al. [46] have modified the method of King and King [47] by a six-term fitting equation based on Debye and Einstein functions as given below:

$$C_{p,m}^0 = 3R \left\{ m \cdot D \frac{\Theta_D}{T} + n \cdot E \frac{\Theta_E}{T} \right\} + A_1 \cdot \frac{T}{K} + A_2 \left(\frac{T}{K} \right)^2 \quad (1)$$

where $D(\Theta_D/T)$ and $E(\Theta_E/T)$ are Debye and Einstein functions, respectively; $m, n, \Theta_D, \Theta_E, A_1$ and A_2 are adjustable parameters; and $(m+n)$ should be close to the number of atoms in the molecule. The linear term in Eq. (1) takes into account the high temperature heat capacity. The heat capacity data shown in Fig. 2 are smoothed using Eq. (1). The fitting parameters are listed in Table 2. The smoothed values of heat capacities of ^nLiH and ^nLiD are shown in Fig. 3. It is evident that, at low enough temperature ($T < 80$ K), the heat capacities of both ^nLiH and ^nLiD are nearly same where as at higher temperatures ($T > 80$ K), the heat capacity of ^nLiD is higher than those of ^nLiH and the difference between their heat capacities remain almost constant above 650 K.

A comparison of the heat capacity results of LiH obtained in this study with those reported in the literature is made in Fig. 4. It can be seen from the figure that, the low temperature heat capacities obtained in this study are in excellent agreement with those of literature [23,45] whereas at higher temperatures substantial deviation is observed from those reported in Ref. [45]. The excellent agreement of low temperature heat capacity obtained in this study with those reported in literature [23,45] is attributed due to the fact that both measurements include direct determination of heat

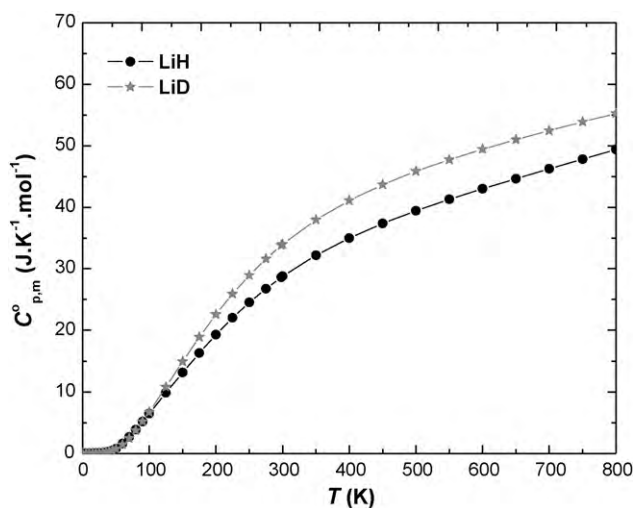


Fig. 3. Smoothed values of heat capacities ($C_{p,m}^0$) of ^nLiH and ^nLiD as a function of temperature obtained from Eq. (1).

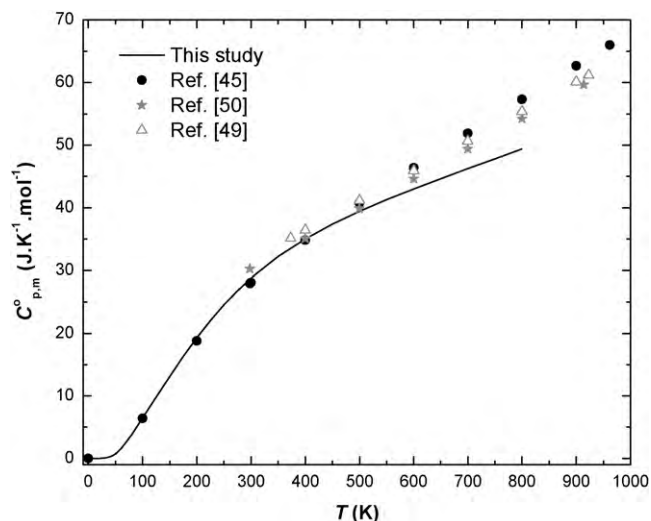


Fig. 4. Comparison of heat capacities of LiH obtained in this study with those reported in literature.

capacity. The deviation of high temperature heat capacity obtained in this study with those reported in literature [45] is attributed due to the fact that the high temperature literature values of heat capacity are derived from enthalpy data. The high temperature data reported in NIST-JANAF thermochemical tables are derived from the enthalpy data determined by Fieldhouse et al. [48] in the temperature range 413.2–914.3 K and by Vogt [49] in the temperature range 878.15–953.15 K. Some high temperature heat capacity data of LiH are also reported in other literature [50,51]. Lang [50] has reported the enthalpy increment of LiH from 300 to 914 K by a second order polynomial equation which on differentiation with respect to temperature gives the heat capacity of LiH in the above temperature range. However, this method gives a linear dependence of heat capacity with temperature in a broad temperature range which is not generally valid for solid materials. Similar linear variation of heat capacity with temperature has been reported by Vogt [49]. All these data are shown in Fig. 4. The heat capacity data obtained in the present study by differential scanning calorimetric method does not show any linear relationship with temperature in the temperature range 298–800 K. Moreover, the data reported in NIST-JANAF table [45] shows a sudden rise in heat capacity above 500 K. In the absence of any valid argument for this sudden rise in heat capacity, we assume the data in our study is more reliable as these are directly measured heat capacity data.

Similarly, the heat capacity data for LiD obtained in the present are in excellent agreement with those reported in the literature [23] in the low temperature region. However, there is no experimental data available in the high temperature region for comparison.

3.3. Construction of thermodynamic tables for ^nLiH and ^nLiD

The smoothed values of heat capacities of ^nLiH and ^nLiD are used to calculate the thermodynamic functions using the method described in an earlier publication [52]. The entropy increment $\{S_m^0(T) - S_m^0(0)\}$ and the enthalpy increment $\{H_m^0(T) - H_m^0(0)\}$ functions have been calculated by numerical integration of the $C_p^0(T)/T$ and $C_p^0(T)$ functions, respectively. These functions have been constructed using polynomial fit of the $C_p^0(T)$ curve in small temperature ranges. The values of $\{H_m^0(T) - H_m^0(298.15 \text{ K})\}$ have been calculated by using the relation:

$$\begin{aligned} \{H_m^0(T) - H_m^0(298.15 \text{ K})\} &= \{H_m^0(T) - H_m^0(0)\} \\ &- \{H_m^0(298.15 \text{ K}) - H_m^0(0)\} \end{aligned} \quad (2)$$

Table 3
Thermodynamic data for ${}^n\text{LiH}$ (s) (w.r.t. standard element reference state).

T/K	$S_m^{\circ}(T)/\text{J K}^{-1} \text{mol}^{-1}$	$C_{p,m}^{\circ}(T)/\text{J K}^{-1} \text{mol}^{-1}$	$H_m^{\circ}(T) - H_m^{\circ}(0)/\text{J mol}^{-1}$	$H_m^{\circ}(T) - H_m^{\circ}(298.15)/\text{J mol}^{-1}$	$-H_m^{\circ}(T)/\text{J mol}^{-1}$	$-C_m^{\circ}(T)/\text{J mol}^{-1}$	$\Phi_m^{\circ}(T)/\text{J K}^{-1} \text{mol}^{-1}$
0	0	0	0				
10	0.0017	0.0037	0.0133				
20	0.0086	0.0211	0.1252				
30	0.0254	0.0748	0.5632				
40	0.0693	0.2719	2.1528				
50	0.1772	0.7625	7.1138				
60	0.385	1.578	18.816				
70	0.705	2.643	39.921				
80	1.135	3.859	72.431				
90	1.663	5.154	117.496				
100	2.273	6.483	175.681				
125	4.07	9.83	379.63				
150	6.14	13.13	666.67				
175	8.40	16.31	1034.7				
200	10.77	19.29	1479.7				
225	13.20	22.04	1996.3				
250	15.65	24.53	2578.4				
275	18.10	26.77	3218.7				
298.15	20.3	28.6	3859.6	0	90,650	96,713	20.3
300	20.5	28.8	3914.2	54.5	90,650	96,805	20.3
350	25.2	32.2	5438.7	1579.0	90,558	99,382	20.7
400	29.7	35.0	7118.7	3259.0	90,310	102,190	21.5
450	34.0	37.4	8927.7	5068.0	89,933	105,217	22.7
500	38.0	39.4	10,847.2	6987.5	89,445	108,451	24.0
550	41.9	41.3	12,864.7	9005.0	88,860	111,882	25.5
600	45.5	43.0	14,971.7	11,112.0	88,185	115,500	27.0
650	49.0	44.6	17,162.7	13,303.0	87,426	119,298	28.6
700	52.4	46.2	19,434.2	15,574.5	86,586	123,268	30.1
750	55.6	47.8	21,786.2	17,926.5	85,666	127,402	31.7
800	58.8	49.4	24,216.7	20,357.0	84,668	131,697	33.3

In order to make full use of the thermodynamic data, $G_m^{\circ}(T)$ should be evaluated which requires a known value of $H_m^{\circ}(0)$. However, absolute value of $H_m^{\circ}(0)$ is difficult to determine or calculate. Therefore, first $H_m^{\circ}(T)$ has been calculated using the relation:

$$H_m^{\circ}(T) = \Delta_f H_{298.15}^{\circ} + \int_{298.15}^T C_{p,m}^{\circ}(T) dT \quad (3)$$

The values of $\Delta_f H_{298.15}^{\circ}$ for ${}^n\text{LiH}$ and ${}^n\text{LiD}$ have been taken as -90.7 and $-91.1 \text{ kJ mol}^{-1}$, respectively from the literature [21].

The absolute value of $S_m^{\circ}(T)$ have been calculated using $S_m^{\circ}(0) = 0$ and the relation:

$$S_m^{\circ}(T) = \int_0^T \frac{C_{p,m}^{\circ}(T)}{T} dT \quad (4)$$

Table 4
Thermodynamic data for ${}^n\text{LiD}$ (s) (w.r.t. standard element reference state).

T/K	$S_m^{\circ}(T)/\text{J K}^{-1} \text{mol}^{-1}$	$C_{p,m}^{\circ}(T)/\text{J K}^{-1} \text{mol}^{-1}$	$H_m^{\circ}(T) - H_m^{\circ}(0)/\text{J mol}^{-1}$	$H_m^{\circ}(T) - H_m^{\circ}(298.15)/\text{J mol}^{-1}$	$-H_m^{\circ}(T)/\text{J mol}^{-1}$	$-C_m^{\circ}(T)/\text{J mol}^{-1}$	$\Phi_m^{\circ}(T)/\text{J K}^{-1} \text{mol}^{-1}$
0	0	0	0				
10	0.0198	0.0279	0.1340				
20	0.0514	0.0716	0.6172				
30	0.0935	0.1485	1.6869				
40	0.1568	0.3223	3.9424				
50	0.2674	0.7256	8.9987				
60	0.461	1.448	19.867				
70	0.758	2.478	39.497				
80	1.169	3.748	70.627				
90	1.692	5.182	115.277				
100	2.316	6.723	174.802				
125	4.22	10.79	393.71				
150	6.56	14.91	714.96				
175	9.15	18.88	1137.3				
200	11.91	22.58	1655.6				
225	14.76	25.94	2262.1				
250	17.65	28.95	2948.2				
275	20.53	31.62	3705.3				
298.15	23.2	33.8	4462.8	0	91,144	98,054	23.2
300	23.4	34.0	4525.5	62.7	91,144	98,160	23.2
350	29.0	37.9	6323.8	1861	91,037	101,162	23.6
400	34.3	41.1	8299.5	3836.7	90,752	104,435	24.6
450	39.2	43.7	10,418.5	5955.7	90,324	107,965	26.0
500	43.9	45.8	12,656.3	81,93.5	89,777	111,737	27.5
550	48.4	47.7	14,995.5	10,532.7	89,129	115,739	29.2
600	52.6	49.4	17,424.1	12,961.3	88,391	119,957	31.0
650	56.6	51.0	19,934.1	15,471.3	87,572	124,382	32.8
700	60.5	52.4	22,520.0	18,057.2	86,678	129,002	34.7
750	64.1	53.9	25,177.8	20,715.0	85,711	133,810	36.5
800	67.6	55.2	27,905.3	23,442.5	84,674	138,798	38.3

Table 5
Debye temperatures of LiH and LiD.

Ref.	Method	Θ_D (K) at 0K	
		LiH	LiD
This study	Debye extrapolation of specific heat	1179 ± 40	1162 ± 30
James and Kheyrandish [10]	Elastic constant data	1128 ± 10	1073 ± 10
Haussuhl and Skorczyk [31]		1128 ± 10	1048 ± 30
Yates et al. [23]	Debye extrapolation of specific heat	1190 ± 80	1030 ± 50
Guinan and Cline [7]	Elastic constant data	1083	1032
Ruffa [16]	Localised continuum model	736	553
Kostiryukov [29]	Specific heat	850	–
Stambaugh and Harris [30]	X-ray data	851	638

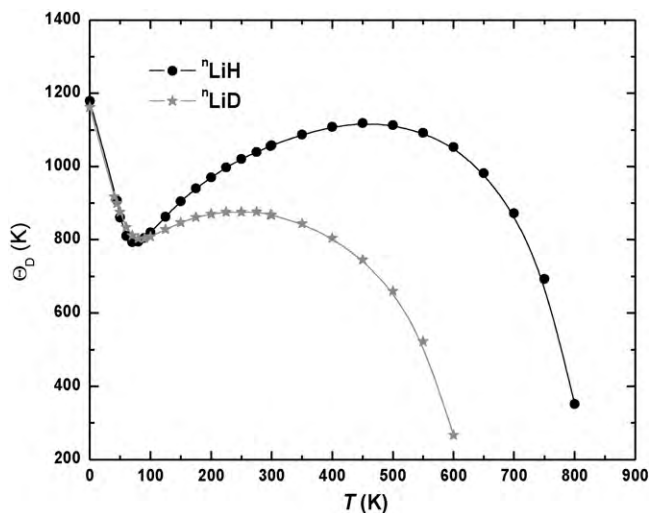


Fig. 5. Plot of Debye temperatures (Θ_D) versus absolute temperature for ${}^7\text{LiH}$ and ${}^7\text{LiD}$.

Now $G_m^o(T)$ can be calculated using the relation:

$$G_m^o(T) = H_m^o(T) - TS_m^o(T) \quad (5)$$

The free energy function (or the Plank's function) $\Phi_m^o(T)$ has been calculated using the relation:

$$\Phi_m^o(T) = - \left\{ \frac{G_m^o(T) - H_m^o(298.15 \text{ K})}{T} \right\} \quad (6)$$

After calculation of all the thermodynamic functions, the values have been tabulated at selected temperatures. The thermodynamic functions which are usually tabulated in the tables are: $C_{p,m}^o$, S_m^o , $\{H_m^o(T) - H_m^o(298.15 \text{ K})\}$, $H_m^o(T)$ and $\Phi_m^o(T)$. The values generated in this study are listed in Tables 3 and 4.

The Debye temperatures (Θ_D) of ${}^7\text{LiH}$ and ${}^7\text{LiD}$ are calculated from the heat capacity data using the tabulated values of Debye function [53]. The variation of Θ_D as a function of absolute temperature for ${}^7\text{LiH}$ and ${}^7\text{LiD}$ are shown in Fig. 5. The values of Θ_D at 0K are found to be 1179 (± 40) and 1162 (± 30)K for ${}^7\text{LiH}$ and ${}^7\text{LiD}$, respectively. The effective Debye temperatures for ${}^7\text{LiH}$ and ${}^7\text{LiD}$ are found to be 1080 and 800 K, respectively. The available literature values of Θ_D along with the data obtained in the present study are listed in Table 5.

4. Conclusions

The heat capacities of ${}^7\text{LiH}$ and ${}^7\text{LiD}$ measured by DSC in the temperature range from 125 to 800 K are found to be in excellent agreement with the reported low temperature heat capacities of ${}^7\text{LiH}$ and ${}^7\text{LiD}$. A six-term equation comprising Debye and Einstein functions was found to suitably fit the heat capacities of ${}^7\text{LiH}$ and ${}^7\text{LiD}$ in the entire temperature range from 0 to 800 K. The smoothed

values of heat capacity were used to calculate various thermodynamic functions for ${}^7\text{LiH}$ and ${}^7\text{LiD}$ from 0 to 800 K. Substantial isotopic effect on heat capacity of ${}^7\text{LiH}$ and ${}^7\text{LiD}$ has been observed at higher temperatures ($>80\text{K}$) whereas below 80 K the isotopic effect is negligible. At all temperatures, the heat capacity of ${}^7\text{LiD}$ is found to be higher than that of ${}^7\text{LiH}$.

References

- [1] F.H. Welch, Nucl. Eng. Des. 26 (1974) 444–460.
- [2] V.G. Plekhanov, Mater. Sci. Eng. R35 (2001) 139–237.
- [3] V.G. Plekhanov, Prog. Solid State Chem. 29 (2001) 71–177.
- [4] A.A. Berezin, A.M. Ibrahim, Mater. Chem. Phys. 19 (1988) 407–430.
- [5] W. Dyck, H. Jex, J. Phys. C: Solid State Phys. 14 (1981) 4193–4215.
- [6] S. Haussuhl, I. Skorczyk, Z. Kristallogr. 130 (1969) 340–345.
- [7] M.W. Guinan, C.F. Cline, J. Nonmetals 1 (1972) 11–15.
- [8] D. Gerlich, C.S. Smith, J. Phys. Chem. Solids 35 (1974) 1587–1592.
- [9] D. Laplaze, M. Boissier, R. Vacher, Solid State Commun. 19 (1976) 445–446.
- [10] B.W. James, H. Kheyrandish, J. Phys. C: Solid State Phys. 15 (1982) 6321–6337.
- [11] A.K.M.A. Islam, M.T. Hoque, IC/94/366.
- [12] W.B. Zimmerman, Phys. Rev. B5 (1972) 4704–4707.
- [13] G.L. Anderson, G. Nasise, K. Philipson, F.E. Pretzel, J. Phys. Chem. Solids 31 (1970) 613–618.
- [14] T.I. Mel'nikova, Teplofiz. Vys. Temp. 18 (1980) 305 (in Russian).
- [15] E.E. Shpil'rain, K.A. Yakimovich, T.N. Mel'nikova, Thermal Properties of Lithium Hydride, Deuteride and Tritide and Their Solutions with Lithium, Energoizdat, Moscow, 1983 (in Russian).
- [16] A.R. Ruffa, Phys. Rev. B 27 (1983) 1321–1325.
- [17] V.I. Tyutyunnik, Phys. Status Solidi B 181 (1994) 373–376.
- [18] V.I. Tyutyunnik, Phys. Status Solidi B 172 (1992) 539–543.
- [19] D.K. Smith, H.R. Leider, J. Appl. Crystallogr. 1 (1968) 246–249.
- [20] R.C. Bowman Jr., J. Phys. Chem. Solids 34 (1973) 1754–1756.
- [21] C.B. Magee, in: W.M. Mueller, et al. (Eds.), Metal Hydrides, Academic Press Inc., New York, 1968 (Chapter 6).
- [22] C.E. Messer, Report NYO-9470, Chemistry, Tufts University, Medford, Massachusetts, 1960.
- [23] B. Yates, G.H. Wostenholm, J.L. Bingham, J. Phys. C: Solid State Phys. 7 (1974) 1769–1778.
- [24] J.I. Lang, Thermodynamic and transport properties of gases, liquids, and solids, in: Symposium on Thermal Properties, Purdue University, ASME, New York, 1959, pp. 405–414.
- [25] J.W. Vogt, USAEC File No. 11888, Tapeo. Div. of Thompson Ramo Wooldridge Inc., 1962.
- [26] C.E. Messer, T.R.P. Gibb, Jr., USAEC Report NYO-8022, Tufts University, 1957.
- [27] A.K.M.A. Islam, Report No. IC/95/119, 1995.
- [28] R.H. Busey, R.B. Bevan, Report No. ORNL 4706, 1971.
- [29] V.N. Kostiryukov, Russ. J. Phys. Chem. 35 (1961) 865.
- [30] C.K. Stambaugh, P.M. Harris, Phys. Rev. 86 (1952) 651.
- [31] S. Haussuhl, W. Skorczyk, Z. Kristallogr. 130 (1969) 340–345.
- [32] J. Boronat, C. Cazorla, D. Colognesi, M. Zoppi, Phys. Rev. B69 (2004) 174302–174309.
- [33] J.P. Vidal, G. Vidal-Valat, Acta Crystallogr. B42 (1986) 131–137.
- [34] P. Loubeyre, R.L. Toullec, M. Hanfland, L. Ulivi, F. Datchi, D. Hausermann, Phys. Rev. B57 (1998) 10403–10406.
- [35] N. Yu, C. Jin, A. Kohlmeyer, J. Phys.: Condens. Matter 19 (2007) 086209–086223.
- [36] J. Hama, N. Kawakami, Phys. Lett. A 126 (1988) 348–352.
- [37] G.D. Barrera, D. Colognesi, P.C.H. Mitchell, A.J. Ramirez-Cuesta, Chem. Phys. 317 (2005) 119–129.
- [38] J. Hama, K. Suito, N. Kawakami, Phys. Rev. B39 (1989) 3351–3360.
- [39] G. Roma, C.M. Bertoni, S. Baroni, Solid State Commun. 98 (1996) 203–207.
- [40] A.K.M.A. Islam, J. Phys. Chem. Solids 55 (1994) 517–521.
- [41] T.A. Dellin, G.J. Dienes, C.R. Fischer, R.D. Hatcher, W.D. Wilson, Phys. Rev. B1 (1970) 1745–1753.
- [42] F.E. Pretzel, G.N. Rupert, C.L. Mader, E.K. Storms, G.V. Gritton, C.C. Rushing, J. Phys. Chem. Solids 16 (1960) 10–20.
- [43] E. Veleckis, J. Phys. Chem. 81 (1977) 526–531.

- [44] C.E. Johnson, R.R. Heinrich, C.E. Crouthamel, *J. Phys. Chem.* 70 (1966) 242–246.
- [45] M.W. Chase, Jr., NIST-JANAF Thermochemical Tables, 4th ed., *J. Phys. Chem. Ref. Data*, Monograph No. 9, 1998.
- [46] B.F. Woodfield, J.B. Goates, J.L. Shapiro, R.L. Putnam, A. Navrotsky, *J. Chem. Thermodyn.* 31 (1999) 245–253.
- [47] K.K. King, E.G. King, Contribution to the data on theoretical metallurgy. Part XIV, Entropies of the elements and inorganic compounds, Bulletin 592 (U.S. Bureau of Mines), 1961.
- [48] I.B. Fieldhouse, J.C. Hedge, J.I. Lang, Armour Research Foundation, PB 151583, 1958.
- [49] J.W. Vogt, Thompson Ramo Wooldridge Inc., Cleveland, Ohio, NASA N63 22167, 1962.
- [50] J.I. Lang, Specific heat of materials, thermodynamic and transport properties of gases, liquids and solids, in: Papers Presented at the Symposium on Thermodynamic Properties, Purdue University, American Society of Mechanical Engineers, New York, 1959, pp. 405–414.
- [51] C.E. Messer, USAEC Report NYO-9470, Tufts University, 1960.
- [52] S.C. Parida, S.K. Rakshit, Z. Singh, *J. Solid State Chem.* 181 (2008) 101–121.
- [53] E.S.R. Gopal, Specific Heats at Low Temperatures, Plenum Press, New York, 1966.